Cell

Mono-Uridylation of Pre-MicroRNA as a Key Step in the Biogenesis of Group II let-7 MicroRNAs

Inha Heo,[1,2,3] Minju Ha,[1,2,3] Jaechul Lim,[1,2] Mi-Jeong Yoon,[2] Jong-Eun Park,[1,2] S. Chul Kwon,[1,2] Hyeshik Chang,[1,2] and V. Narry Kim[1,2,*]
[1]Institute for Basic Science
[2]School of Biological Sciences
Seoul National University, Seoul 151-742, Korea
[3]These authors contributed equally to this work
*Correspondence: narrykim@snu.ac.kr
http://dx.doi.org/10.1016/j.cell.2012.09.022

SUMMARY

RNase III Drosha initiates microRNA (miRNA) maturation by cleaving a primary miRNA transcript and releasing a pre-miRNA with a 2 nt 3′ overhang. Dicer recognizes the 2 nt 3′ overhang structure to selectively process pre-miRNAs. Here, we find that, unlike prototypic pre-miRNAs (group I), group II pre-miRNAs acquire a shorter (1 nt) 3′ overhang from Drosha processing and therefore require a 3′-end mono-uridylation for Dicer processing. The majority of let-7 and miR-105 belong to group II. We identify TUT7/ZCCHC6, TUT4/ZCCHC11, and TUT2/PAPD4/GLD2 as the terminal uridylyl transferases responsible for pre-miRNA mono-uridylation. The TUTs act specifically on dsRNAs with a 1 nt 3′ overhang, thereby creating a 2 nt 3′ overhang. Depletion of TUTs reduces let-7 levels and disrupts let-7 function. Although the let-7 suppressor, Lin28, induces inhibitory oligo-uridylation in embryonic stem cells, mono-uridylation occurs in somatic cells lacking Lin28 to promote let-7 biogenesis. Our study reveals functional duality of uridylation and introduces TUT7/4/2 as components of the miRNA biogenesis pathway.

INTRODUCTION

Biogenesis of microRNA (miRNA) involves multiple maturation steps (Kim et al., 2009). As miRNA sequences are embedded in the stem of a local hairpin in a nascent transcript (primary miRNA [pri-miRNA]), a couple of endonucleolytic reactions are needed to yield a functional miRNA. The nuclear RNase III Drosha initiates the maturation process by cleaving a pri-miRNA to release an ~70 nt hairpin-shaped RNA (pre-miRNA) (Lee et al., 2003). Together with its cofactor DGCR8 (also known as Pasha), Drosha cuts the hairpin at 11 bp away from the base of the hairpin (Denli et al., 2004; Gregory et al., 2004; Han et al., 2004, 2006; Landthaler et al., 2004). Like other RNase-III-type endonucleases, Drosha introduces a staggered cut such that the product acquires a characteristic 2 nt overhang at the 3′ terminus. After cleavage, the pre-miRNA is exported to the cytoplasm by exportin 5 in a complex with Ran-GTP (Bohnsack et al., 2004; Lund et al., 2004; Yi et al., 2003). The cytoplasmic RNase III Dicer processes the pre-miRNA further to liberate a small RNA duplex (Bernstein et al., 2001; Grishok et al., 2001; Hutvágner et al., 2001; Ketting et al., 2001; Knight and Bass, 2001). Human Dicer binds to the pre-miRNA with a preference for the 2 nt 3′ overhang (Zhang et al., 2004). The 5′ and 3′ ends of pre-miRNA are accommodated in two basic pockets (5′ and 3′ pockets, respectively) located in the PAZ domain of Dicer (Park et al., 2011). Dicer measures 22 nt from the 5′ phosphorylated end of pre-miRNA and cleaves near the terminal loop (Park et al., 2011; Vermeulen et al., 2005; Zhang et al., 2002, 2004). The resulting small RNA duplex is loaded on to Argonaute and one of the strands is selected to form an active RNA-induced silencing complex (RISC) (Hammond et al., 2001; Mourelatos et al., 2002; Tabara et al., 1999).

The let-7 miRNA family is highly conserved throughout bilaterian animals (Pasquinelli et al., 2000; Reinhart et al., 2000; Roush and Slack, 2008). Let-7 miRNAs suppress cell proliferation and promote cell differentiation by targeting multiple genes including HMGA2, RAS, and Lin28 (Büssing et al., 2008). At the organismal level, let-7 has been implicated in multiple processes such as larval development in *Caenorhabditis elegans* and growth and glucose metabolism in mammals (Grosshans et al., 2005; Meneely and Herman, 1979; Pasquinelli et al., 2000; Reinhart et al., 2000; Zhu et al., 2010, 2011). Biogenesis of let-7 is suppressed in embryonic stage and in certain cancer cells (Büssing et al., 2008). We and other groups have previously shown that let-7 maturation is inhibited by an RNA-binding protein Lin28 (Heo et al., 2008; Newman et al., 2008; Rybak et al., 2008; Viswanathan et al., 2008). There are two paralogues of Lin28 (Lin28A and Lin28B) in mammals that are biochemically similar but are distinct in expression patterns and subcellular localization (Balzer and Moss, 2007; Guo et al., 2006; Piskounova et al., 2011; Polesskaya et al., 2007; Richards et al.,

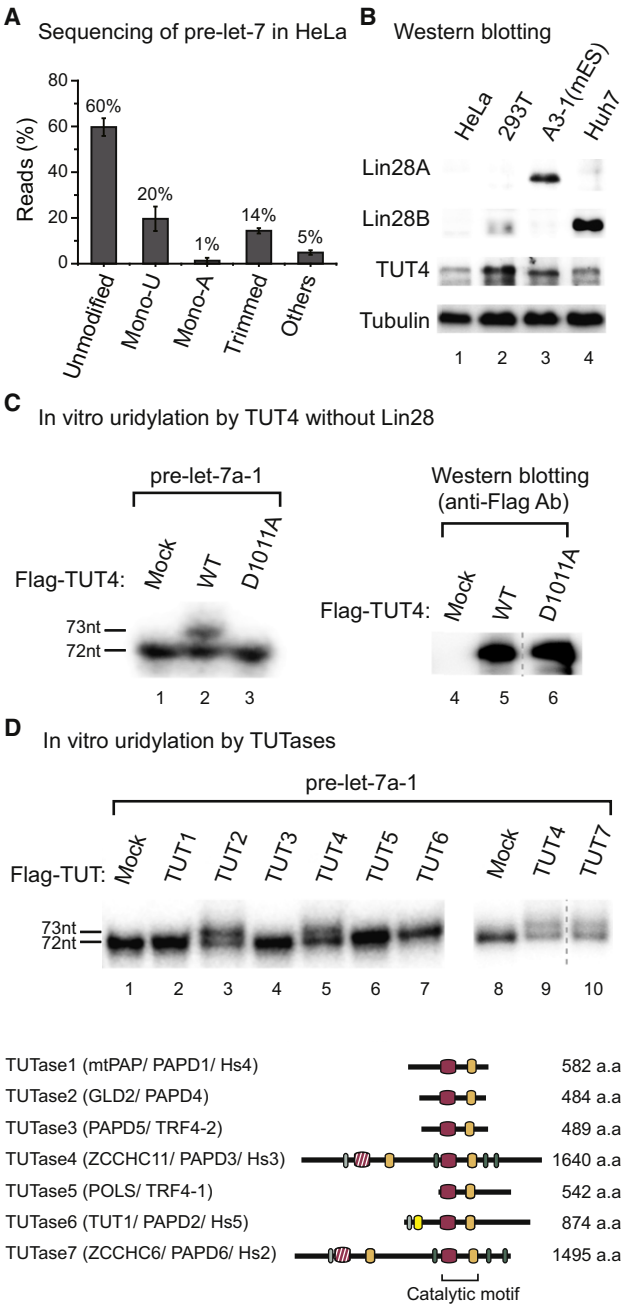

Figure 1. Pre-let-7 Is Mono-Uridylated in the Absence of Lin28

(A) Significant amount of pre-let-7 carries an untemplated uridine at its 3′ end (Mono-U). A total of 145 pre-let-7 clones were obtained from two independent experiments by using HeLa cells (see Figure S1A for details). "Trimmed" reads are shorter than pre-let-7 and "others" reads do not belong to any other categories (see Table S1). Error bars indicate SD.

(B) Expression pattern of Lin28A, Lin28B, and TUT4 in HeLa (human cervical adenocarcinoma), 293T (human embryonic kidney), A3-1 (mouse embryonic stem cell), and Huh7 (human hepatocellular carcinoma). Tubulin was detected as a loading control.

(C) TUT4 catalyzed mono-uridylation of pre-let-7a-1 in the absence of Lin28 (left). Immunopurified wild-type or catalytically dead mutant (D1011A) TUT4 was incubated with 5′ end-labeled pre-let-7a-1 and 0.25 mM UTP. (right) Comparable amounts of proteins were used in the reaction.

(D) Not only TUT4 but also TUT7 and TUT2 mono-uridylate pre-let-7a-1 (top). In vitro uridylation was performed by using immunopurified human TUTases (TUTs). The levels of immunoprecipitated TUTs are shown in Figure S1B. Bottom: domain organization of human TUTs. (red, nucleotidyl transferase domain; orange, PAP-associated domain; hatched red, inactive nucleotidyl transferase domain due to sequence variations; light green, C2H2 zinc finger domain; green, CCHC zinc finger domain; yellow, RNA recognition motif). Dashed line indicates discontinuous lanes from the same gel.

2004; Yang and Moss, 2003). Lin28A is expressed in embryonic cells and cancer cells and localized mainly in the cytoplasm, whereas Lin28B is induced in cancer cells that do not express Lin28A and is predominantly located in the nucleolus. The Lin28 proteins bind to the terminal loop of let-7 precursors through a conserved motif GGAG to interfere with Drosha and Dicer processing (Heo et al., 2009; Loughlin et al., 2012; Nam et al., 2011). Lin28 also interacts with terminal uridylyl transferase 4 (TUT4, also known as ZCCHC11, PAPD3, and Hs3) to induce oligo-uridylation (10–30 nt) of pre-let-7 by TUT4 (Hagan et al., 2009; Heo et al., 2009). TUT7 (also known as ZCCHC6, PAPD6, and Hs2) has a similar but weaker activity compared to that of TUT4 (Heo et al., 2009). Because Dicer disfavors a substrate with such a long single-stranded RNA tail, oligo-uridylation provides an effective way of suppressing let-7 maturation. Uridylation has also been associated with RNA degradation and the U tails are thought to facilitate the recruitment of exonucleases (Ji and Chen, 2012; Kim et al., 2010; Ren et al., 2012; Wickens and Kwak, 2008; Wilusz and Wilusz, 2008; Zhao et al., 2012).

Recent high-throughput studies of miRNA population in various cell types suggested that miRNAs and their precursors may undergo multiple types of posttranscriptional modifications (Burroughs et al., 2010; Chiang et al., 2010; Jones et al., 2009; Newman et al., 2011; Wu et al., 2009; Wyman et al., 2011). However, most modification events appear to be rare and their functional relevance remains unclear. In the current study, we find that certain pre-miRNAs are frequently mono-uridylated and that the uridylating enzymes play critical roles in the maturation and function of miRNAs.

RESULTS

Mono-Uridylation of Pre-let-7 in the Absence of Lin28

To investigate posttranscriptional regulation of miRNAs at the pre-miRNA level, we cloned and sequenced pre-let-7 from HeLa cells (Figure S1A available online). To our surprise, a considerable portion of the pre-let-7 clones (20%) carried one untemplated uridyl residue at the 3′ end (Figure 1A). Because HeLa cells do not express Lin28A or Lin28B (Figure 1B), this result indicates that pre-let-7 may undergo uridylation even in the absence of Lin28. Other modifications appear to be rare events: only 1% carried an untemplated adenosine and there was no clone with extra guanosine or cytidine (Figure 1A and Table S1). Most of the remaining clones were shorter than pre-let-7, likely representing degradation intermediates.

We refer to the nontemplated addition of a single uridine as "mono-uridylation" because the length of the U tail is clearly distinct from that in "oligo-uridylation" (10–30 nt) observed in

Lin28-expressing cells (Hagan et al., 2009; Heo et al., 2008, 2009). In a recent report, Hammond and colleagues made a similar observation of mono-uridylation in various cell types (Newman et al., 2011). A caveat of ours and Hammond group's findings, however, is that only the steady-state levels were examined. Thus, it is unclear from these data whether the mono-uridylated pre-miRNAs are active precursors to be processed or they are nonfunctional dead-end products facing degradation.

TUT7, TUT4, and TUT2 Mono-Uridylate Pre-let-7 In Vitro

To understand the functional significance of mono-uridylation, it was critical for us to identify the factors responsible for the modification. Interestingly, from in vitro uridylation assay, we noticed that TUT4 has a mono-uridylating activity in the absence of Lin28 (Figure 1C), whereas the same enzyme catalyzes oligo-uridylation when Lin28 is bound (Heo et al., 2009). We detected pre-let-7a-1 extended by 1 nt when 5′ end-labeled pre-let-7a-1 was incubated with wild-type TUT4 but not with a catalytically dead mutant (D1011A) (Figure 1C). Consistent with this result, TUT4 interacts with pre-let-7 even in the absence of Lin28, albeit transiently, as recently shown by single-molecule detection technique called SIMPlex (Yeom et al., 2011). The duration of the interaction between TUT4 and pre-let-7 is very short (1.1 ± 0.2 s), explaining why we previously failed to detect the interaction in bulk binding assays (Heo et al., 2009).

We further examined other terminal uridylyl transferases (TUTases or TUTs, also called poly [U] polymerases) for their activity toward pre-let-7 (Martin and Keller, 2007; Stevenson and Norbury, 2006; Wilusz and Wilusz, 2008). We immunoprecipitated seven TUTases (TUT1, TUT2, TUT3, TUT4, TUT5, TUT6, and TUT7) for in vitro uridylation experiments (Figures 1D and S1B). Interestingly, TUT7 and TUT2 as well as TUT4 can catalyze mono-uridylation of pre-let-7a-1 (Figure 1D). Such mono-uridylation activity was not detected when point mutants of the conserved catalytic site in TUT7 (D1060A) or TUT2 (D215A) were used (Figures S1C and S1D), excluding the possibility that the observed activity is due to contamination of another enzyme. When we substituted UTP with other NTPs, TUT7 and TUT4 failed to utilize other NTPs, whereas TUT2 incorporated ATP and GTP as well as UTP (Figure S1E). Thus, TUT7 and TUT4 are specific to uridylyl transfer, whereas TUT2 has a broader nucleotide usage.

TUT7 is closely related to TUT4 (Figure 1D), but its oligo-uridylation activity for pre-let-7 is lower compared to that of TUT4 (Heo et al., 2009). It was unexpected that TUT2 (also known as GLD2 and PAPD4) has uridylating activity and acts on a pre-miRNA. TUT2 is known to induce translation by poly-adenylating mRNAs at synapses (Rouhana et al., 2005) and during oogenesis (Nakanishi et al., 2006). In addition, TUT2 mono-adenylates and stabilizes mature miR-122 in mammalian liver cells and fibroblasts (Burns et al., 2011; Katoh et al., 2009).

TUT7, TUT4, and TUT2 Promote let-7 Biogenesis in Cells

We next asked whether TUT7, TUT4, and TUT2 (TUT7/4/2) have any effect on let-7 biogenesis by transfecting siRNAs against the TUTs into HeLa cells. Western blotting confirmed the depletion of each protein (Figure 2A). An individual knockdown of TUTs induced marginal alteration at the levels of mature and pre-let-7 (Figure 2B, lanes 3-5). Because our uridylation assay by using immunoprecipitates indicated that TUT7/4/2 have similar activities (Figure 1D), we reasoned that the three TUTs may function redundantly in cells. Consistent with this notion, when all the three TUTs were depleted simultaneously with a mixture of three siRNAs (siTUT mix), pre-let-7 increased significantly, whereas mature let-7 decreased (Figures 2B, lane 2, and 2C). Of note, the let-7a probe may cross-hybridize to other let-7 members because of sequence similarities. Our result indicates that let-7 maturation was blocked at the pre-let-7 level after depletion of TUTs. Unlike let-7, the change in miR-16 level was insignificant in TUT-depleted cells (Figures 2B lane 8, and 2C), implicating that TUT7/4/2 may contribute specifically to let-7 maturation. Similar observations were made with two additional sets of siRNA mixtures against TUT7/4/2, ruling out a possibility of off-target effects (Figures S2A–S2C). Notably, the impact of TUT knockdown on let-7 was as strong as that of Dicer (Figures 2B, 2C, S2E and S2F), which indicates that TUT7/4/2 may play an integral role in let-7 biogenesis.

Combinatorial knockdown of two TUTs (siTUT7&4, siTUT7&2, and siTUT4&2) resulted in similar but less prominent effects on let-7 maturation compared to that of TUT7/4/2 (siTUT mix) (Figures S2D–S2F). Thus, all the three TUTs may act redundantly in let-7 biogenesis. It is noted that TUT7 depletion in single- or double-knockdown experiments affected let-7 maturation modestly but significantly, whereas that of TUT4 and TUT2 had less obvious effects (Figures 2C, S2E and S2F). These data implicate that TUT7 may be the major enzyme for pre-let-7 mono-uridylation although we cannot rule out the possibility that TUT4 or TUT2 may function dominantly in other cell types.

TUT7, TUT4, and TUT2 Are Required for Pre-let-7 Mono-Uridylation in Cells

To investigate the uridylation status of pre-let-7 in HeLa cells depleted of TUT7/4/2, we performed sequencing of pre-let-7 (Figure 2D). The portion of mono-uridylated pre-let-7 (let-7a-1, d, f-1, f-2, and g) decreased markedly (from 20% to 3%) in siTUT mix-treated cells. This result clearly demonstrates that TUT7/4/2 are indeed required for mono-uridylation of pre-let-7 in cells.

Interestingly, the trimmed forms of pre-let-7 (mostly 1 nt shorter at the 3′ end than unmodified pre-let-7) increased considerably upon TUT knockdown (Figure 2D and Table S1), suggesting that mono-uridylation may protect pre-miRNA from 3′-exonuclease-mediated trimming. Because the 3′ trimming enzyme for mammalian miRNA is unknown, it is currently unclear by which mechanism pre-miRNAs are degraded and how mono-uridylation influences trimming.

Mono-Uridylation of Pre-let-7 Enhances Dicer Processing

How does mono-uridylation promote let-7 biogenesis? We found that pre-let-7a-1 has an unusual end structure: a 1 nt 5′ overhang and a 2 nt 3′ overhang (Figure 3A, unmodified). Because this structure is equivalent to a 1 nt 3′ overhang as far as Dicer processing is concerned (Park et al., 2011), it is expected that pre-let-7a-1 is a suboptimal substrate for Dicer.

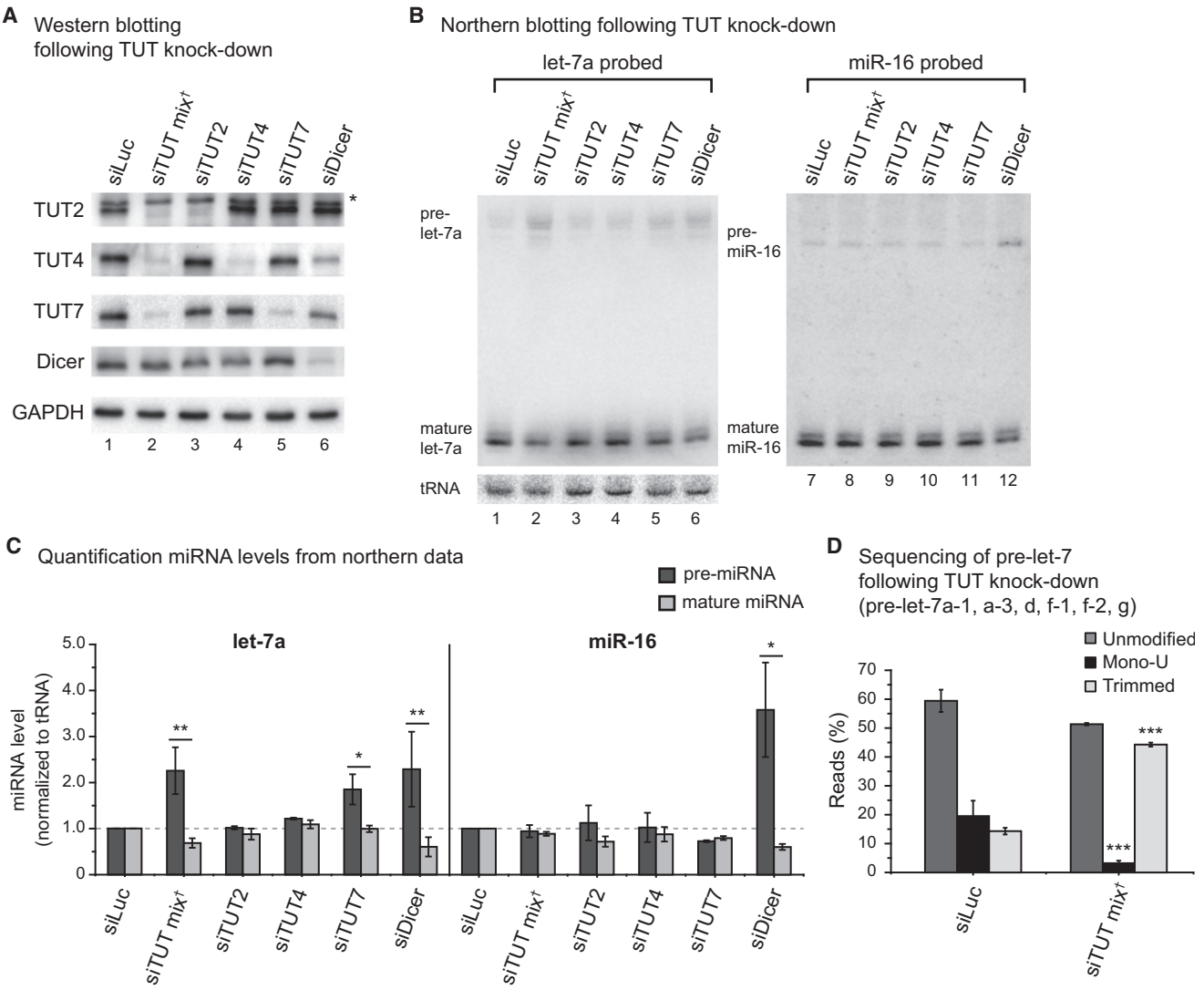

Figure 2. TUT7, TUT4, and TUT2 Redundantly Promote Biogenesis of let-7

(A) TUT7, TUT4, and TUT2 proteins were depleted in HeLa cells. GAPDH was detected as a loading control. An asterisk indicates a nonspecific band.

(B) Concurrent knockdown of TUT7, TUT4, and TUT2 increased pre-let-7a levels, whereas decreasing mature let-7a levels (left). The same membrane was probed for miR-16 (right). tRNA-lys was detected as a loading control.

(C) The levels of mature and precursor of let-7a (left) and miR-16 (right) were quantified from two independent northern blot experiments that include the data shown in (B) and normalized against tRNA levels. Error bars indicate SDs. Paired one-tailed t test was used to calculate the statistical significance of decrease in the ratio of mature to pre-let-7a level (*$p < 0.05$, **$p < 0.01$). See also Figure S2.

(D) Pre-let-7 was sequenced following the knockdown of TUTs (Figure S1A). A proportion of mono-uridylated pre-let-7 significantly decreased in TUT-depleted HeLa cells (***$p < 0.001$, Fisher's exact test). Percentages of each let-7 population were calculated from biological duplicates (Table S1). Error bars indicate SDs. †: siTUT mix represents a mixture of equal amounts of siTUT7, siTUT4, and siTUT2, which applies for all figures.

This unusual end structure is generated by Drosha cleavage (not by trimming), which we confirmed by performing in vitro Drosha processing of pri-let-7 and cloning the products from the reaction (Figure S3). Given that a 2 nt 3′ overhang of pre-miRNA is favored by Dicer (Park et al., 2011; Zhang et al., 2004), we expected that mono-uridylation of pre-let-7 would create an optimal substrate for Dicer processing (Figure 3A, mono-U). Consistent with our prediction, in vitro assay with immunopurified human Dicer demonstrated clearly that mono-uridylated pre-let-7a-1 is processed more efficiently than the unmodified counterpart (Figure 3B). Another family member, pre-let-7b, gave a similar but more dramatic result (Figures 3C and D). Mono-uridylated pre-let-7b was cleaved by Dicer efficiently, whereas unmodified counterpart was barely processed in our assay, which clearly shows that mono-uridylation is necessary for efficient Dicer processing (Figure 3D). Taken together with the results from the knockdown experiments (Figure 2), our data indicate that mono-uridylation of pre-let-7

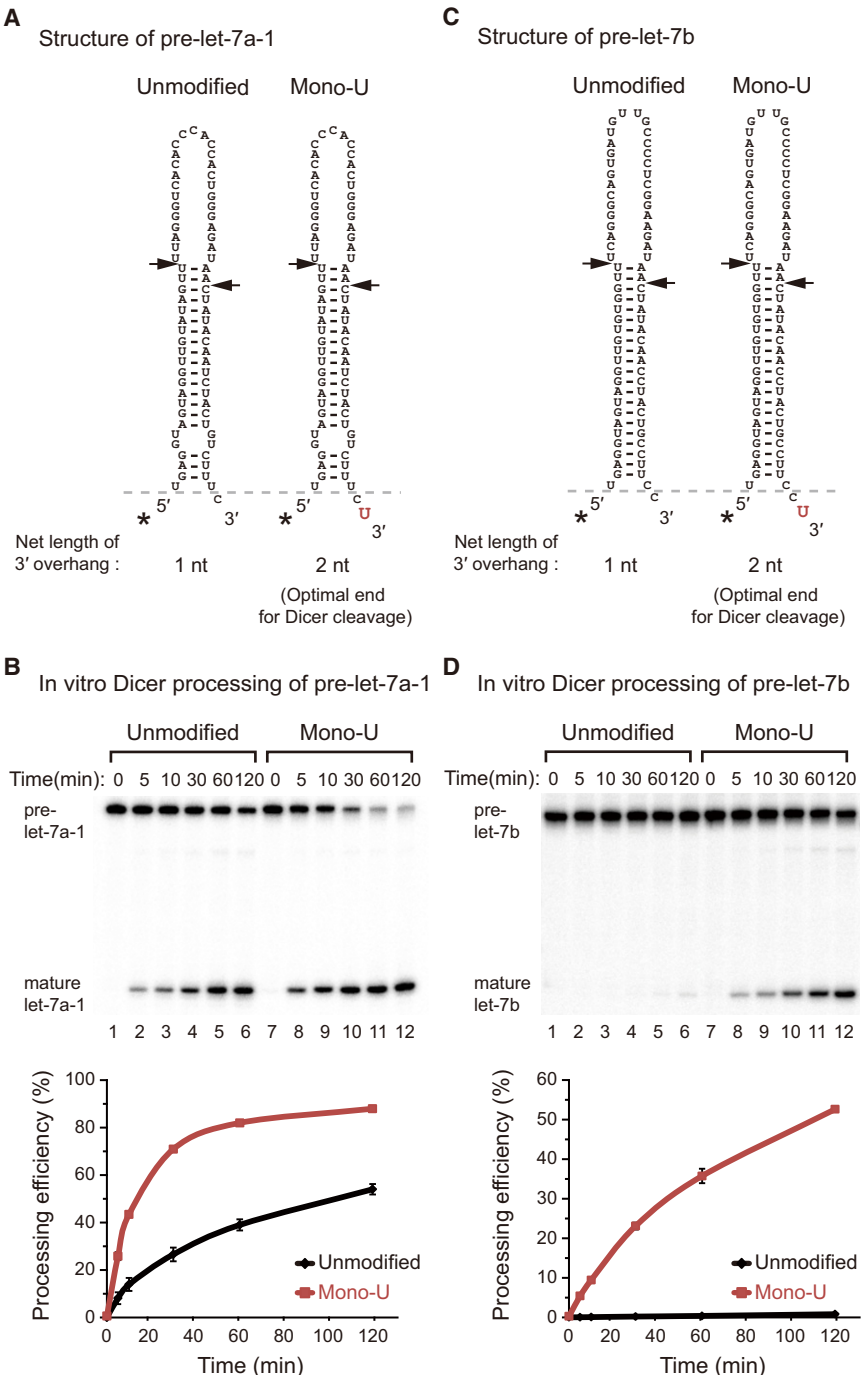

Figure 3. Mono-Uridylation of Pre-let-7 Enhances Dicer Processing

(A and C) Shown are the structures of human pre-let-7a-1 and pre-let-7b. Mono-uridylation makes pre-let-7 an optimal substrate for Dicer cleavage by elongating the overhang from 1 nt to 2 nt. Arrows indicate Dicer processing sites and untemplated uridine addition is represented in red. See also Figure S3.

(B and D) Mono-uridylated pre-let-7a-1 or pre-let-7b was processed more efficiently by purified Dicer than their unmodified counterparts. Processing efficiency was measured from two independent experiments. Error bars indicate SDs.

by TUT7/4/2 promotes let-7 biogenesis by enhancing Dicer processing.

The let-7 Family Is Subdivided into Two Groups Based on the End Structure of the Precursor

In humans, nine distinct let-7 members are generated from 12 different precursors. To see whether all let-7 members are regulated by the same mechanism, we examined the end structure of let-7 precursors (Figures 4A and S4A). We inferred the 3′ end of pre-let-7 based on the 3′ end of mature let-7-3p sequences from multiple small RNA deep sequencing data (See Experimental Procedures for details). In the case of let-7a-1 and let-7d, we performed in vitro Drosha processing and cloned the products in order to annotate the exact Drosha cleavage sites (Figure S3). Based on these analyses, we redetermined the 3′ end of several let-7 precursors (let-7b, c, d, f-1, f-2, i, and miR-98) that appear to be misannotated in miRBase database. By analyzing the end structure of precursor, we found that three let-7 sisters (let-7a-2, c, and e) are predicted to carry a typical end structure (2 nt 3′ overhang) as seen in most other pre-miRNAs outside the let-7 family (Figures 4A and S4A). We refer to this prototypic subset as "group I." On the other hand, the precursors of nine let-7 miRNAs (let-7a-1, a-3, b, d, f-1, f-2, g, i, and miR-98) have a 1 nt 3′ overhang. We name this unusual class as "group II" (Figures 4A and S4A). The pri-miRNAs of group II let-7 contain a bulged uridine (adenosine in the case of let-7d) next to Drosha processing site. It is likely that Drosha does not recognize this bulged nucleotide, which is expected to loop out without disrupting the stem, as often found in structural studies on small bulges in dsRNA (Tian et al., 2004). Thus, Drosha processing of a group II pri-miRNA would result in a 1 nt 5′ overhang (the bulged uridine) and a 2 nt 3′ overhang, which, together, is equivalent to a 1 nt 3′ overhang structure.

When we examined the let-7-3p reads from small RNA deep sequencing libraries from various human tissues (listed in Table S2), in the case of group II let-7, mono-uridylated let-7-3p was more abundant than the unmodified let-7-3p (Figures 4B and S4B). For group I let-7, however, the unmodified

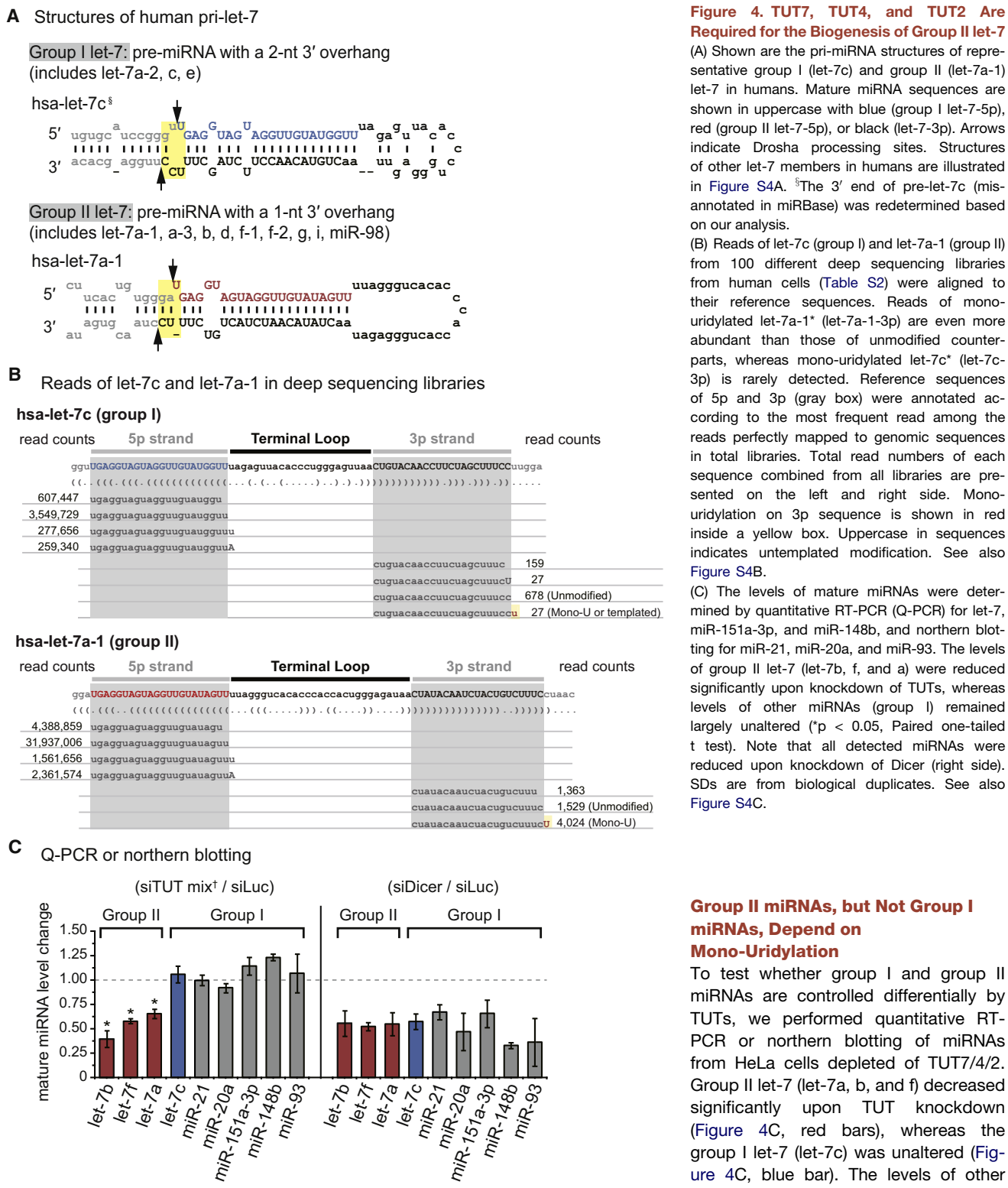

Figure 4. TUT7, TUT4, and TUT2 Are Required for the Biogenesis of Group II let-7

(A) Shown are the pri-miRNA structures of representative group I (let-7c) and group II (let-7a-1) let-7 in humans. Mature miRNA sequences are shown in uppercase with blue (group I let-7-5p), red (group II let-7-5p), or black (let-7-3p). Arrows indicate Drosha processing sites. Structures of other let-7 members in humans are illustrated in Figure S4A. §The 3′ end of pre-let-7c (misannotated in miRBase) was redetermined based on our analysis.

(B) Reads of let-7c (group I) and let-7a-1 (group II) from 100 different deep sequencing libraries from human cells (Table S2) were aligned to their reference sequences. Reads of mono-uridylated let-7a-1* (let-7a-1-3p) are even more abundant than those of unmodified counterparts, whereas mono-uridylated let-7c* (let-7c-3p) is rarely detected. Reference sequences of 5p and 3p (gray box) were annotated according to the most frequent read among the reads perfectly mapped to genomic sequences in total libraries. Total read numbers of each sequence combined from all libraries are presented on the left and right side. Mono-uridylation on 3p sequence is shown in red inside a yellow box. Uppercase in sequences indicates untemplated modification. See also Figure S4B.

(C) The levels of mature miRNAs were determined by quantitative RT-PCR (Q-PCR) for let-7, miR-151a-3p, and miR-148b, and northern blotting for miR-21, miR-20a, and miR-93. The levels of group II let-7 (let-7b, f, and a) were reduced significantly upon knockdown of TUTs, whereas levels of other miRNAs (group I) remained largely unaltered (*$p < 0.05$, Paired one-tailed t test). Note that all detected miRNAs were reduced upon knockdown of Dicer (right side). SDs are from biological duplicates. See also Figure S4C.

let-7-3p was dominant (Figures 4B and S4B). These data suggest that mono-uridylation may be required specifically for group II let-7 members.

Group II miRNAs, but Not Group I miRNAs, Depend on Mono-Uridylation

To test whether group I and group II miRNAs are controlled differentially by TUTs, we performed quantitative RT-PCR or northern blotting of miRNAs from HeLa cells depleted of TUT7/4/2. Group II let-7 (let-7a, b, and f) decreased significantly upon TUT knockdown (Figure 4C, red bars), whereas the group I let-7 (let-7c) was unaltered (Figure 4C, blue bar). The levels of other group I miRNAs (miR-21, miR-20a, miR-151a-3p, miR-148b, and miR-93) did not change in the TUT knockdown sample (Figure 4C, gray bars). Our data indicate that TUT7/4/2 play a critical role in the biogenesis of group II let-7.

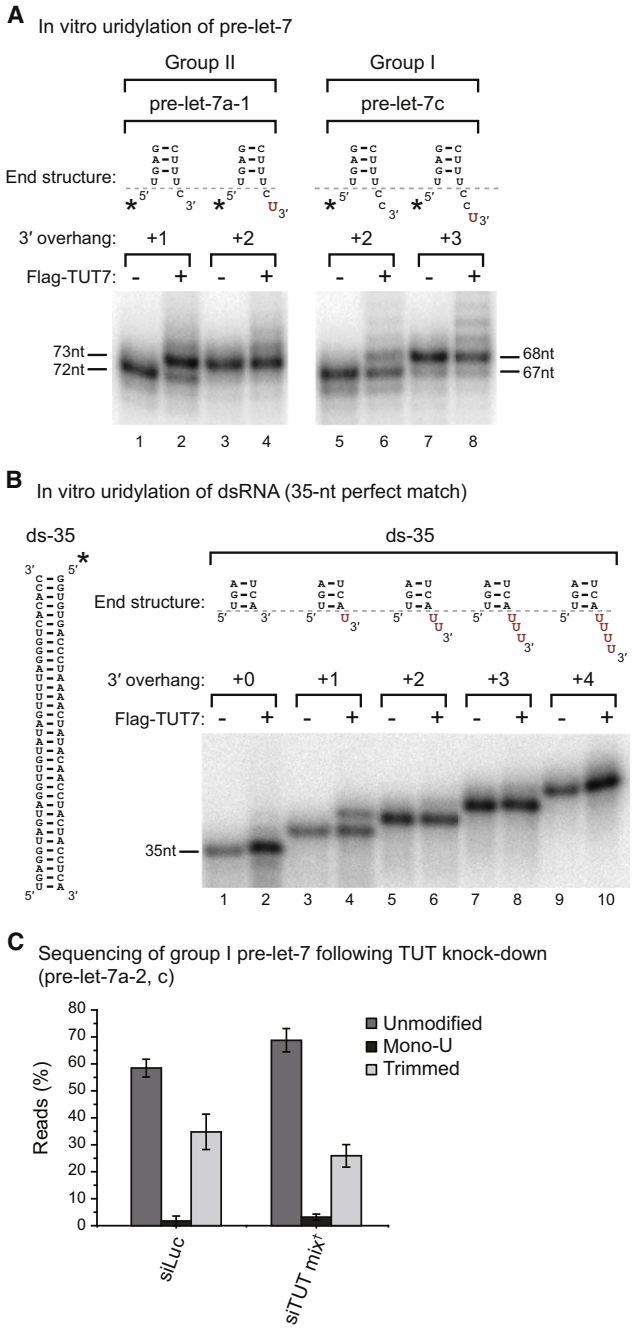

Figure 5. TUTs Act Specifically on dsRNAs with a 1 nt 3′ Overhang

(A) Unmodified pre-let-7a-1 bearing a 1 nt 3′ overhang (group II) underwent mono-uridylation more efficiently than pre-let-7c (group I) and their mono-uridylated variants. In vitro uridylation assay was performed by incubating immunopurified TUT7 with 5′-end labeled RNA. See also Figure S5.

(B) The optimal substrate for mono-uridylation of TUT are dsRNAs with a 1 nt 3′ overhang. Immunopurified TUT7 was incubated with dsRNAs (ds-35) carrying an extra 3′ tail of different lengths. An asterisk indicates a radio-labeled phosphate.

(C) Cloning of group I pre-let-7 shows that only a small portion of group I pre-let-7 carries an extra uridine in HeLa cells (2%, 2 out of 99) (see also Figure S1A). Percentages of each let-7 population were calculated from biological duplicates (Table S4). Error bars indicate SDs.

We also performed small RNA deep sequencing to investigate the global changes of miRNA upon knockdown of TUTs (Figure S4C and Table S3). Consistent with the quantitative RT-PCR result, all of the group II let-7 decreased after depletion of TUT7/4/2, whereas group I let-7 remained unchanged or modestly increased. It is noted that some of the group I miRNAs appeared to have been affected by TUT depletion in deep sequencing data (e.g., miR-21 and miR-93 in Figure S4C) although we could not confirm such changes by quantitative RT-PCR and northern blotting (Figure 4C), indicating that our sequencing data may not have been highly quantitative. Nevertheless, our results collectively demonstrate that TUT7/4/2 are required specifically for the biogenesis of group II let-7.

Note that we classified let-7a (which are produced from three loci, let-7a-1, a-2, and a-3) as group II miRNA in Figures 4C and S4C because the contribution of let-7a-2 (group I) to total let-7a population is expected to be trivial (~1%), judging from the relative abundance of let-7a-2* compared to let-7a-1*/3* from small RNA sequencing data in HeLa cells (data not shown).

TUTs Specifically Mono-Uridylate Group II miRNA

In order to understand the mechanism underlying the specificity of uridylation, we compared a group II precursor (let-7a-1) and a group I precursor (let-7c) in uridylation assay. Interestingly, pre-let-7a-1 was mono-uridylated more efficiently than pre-let-7c (Figure 5A, lanes 1 and 2 and lanes 5 and 6). Another group II miRNA, pre-let-7b, was also mono-uridylated with higher efficiency compared to pre-let-7c (Figure S5A, lane 1 and 2 and lanes 7 and 8). Thus, TUT7 acts selectively on group II pre-miRNAs.

We hypothesized that TUT7 may discriminate the substrates based on the 3′ overhang structure. Consistent with this notion, mono-uridylated pre-let-7a-1 was not uridylated efficiently by TUT7 (Figure 5A, lanes 3 and 4), indicating that TUT7 recognizes the 3′ overhang and transfers one uridylyl residue only when the pre-existing overhang is 1 nt in net length. Mono-uridylated pre-let-7a-1 may not be extended further because a 2 nt 3′ overhang is disfavored by TUT7. TUT4 and TUT2 also showed similar preference for unmodified pre-let-7a-1 (with 1 nt 3′ overhang) compared to its mono-uridylated counterpart (with 2 nt 3′ overhang) (Figures S5B and S5C). To further validate our hypothesis, we incubated immunopurified TUT7 with dsRNAs containing 3′ overhang of variable length (0 to 4 nt). Interestingly, only the substrate with 1 nt 3′ overhang was significantly mono-uridylated (Figure 5B, lane 4). Our results demonstrate that TUT7 specifically recognizes dsRNAs with 1 nt 3′ overhang to generate an optimal substrate for Dicer.

Consistently, when we cloned precursors of group I miRNAs (pre-let-7c and a-2), we found that only 2% of the precursors have an extra U at the 3′ end and that the U residue is genome templated (Figure 5C and Table S4). Furthermore, the proportion of mono-uridylated group I let-7 was not reduced in TUT-depleted cells (Figure 5C), indicating that mono-uridylation of group I is a rare event, if any.

Functional Significance and Evolutionary Conservation of Group II let-7

Group II let-7 is expressed more abundantly than group I let-7 in HeLa cells (accounting for 98% of total let-7 reads) (Table S3).

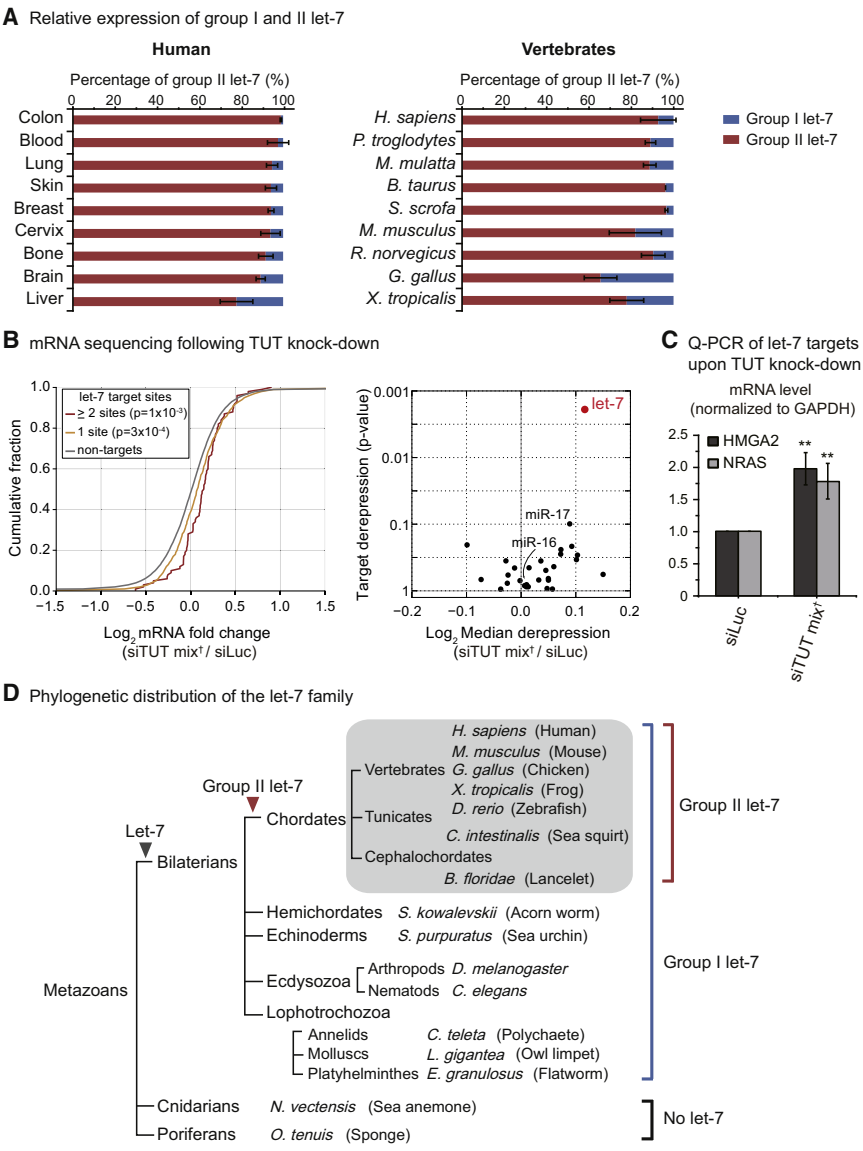

Figure 6. Mono-Uridylation Is Critical for Functionality of Group II let-7

(A) Group II let-7 miRNAs are expressed predominantly in most human cells as well as in other vertebrates. Let-7 reads were analyzed in sequencing libraries from 104 different human cells (from nine distinct organs) and from various tissues of vertebrate species (listed in Table S2). Average percentages are presented with error bars corresponding to SDs. Number of libraries used: blood, 37; colon, 2; lung, 2; cervix, 14; skin, 25; breast, 3; bone, 2; brain, 4; liver, 15; *H. sapiens*, 104; *Pan troglodytes*, 3; *Macaca mulatta*, 3; *Bos taurus*, 1; *Sus scrofa*, 7; *M. musculus*, 75; *Rattus norvegicus*, 16; *G. gallus*, 2; *X. tropicalis*, 2.

(B) Let-7 target genes were specifically derepressed in mRNA deep sequencing from TUT-depleted HeLa cells. (left) Shown is the cumulative distribution of mRNA changes. Two-sided Kolmogorov-Smirnov test was used to calculate the statistical significance of mRNA derepression. (right) The x axis represents a median derepression of mRNAs that contain target sites of each miRNA. The y axis represents a significance of mRNA derepression calculated by using two-sided Kolmogorov-Smirnov test. Target genes with 7-mer and 8-mer sites were predicted from TargetScan human release 6.1.

(C) Q-PCR showed that mRNA levels of HMGA2 and NRAS, targets of let-7, accumulated significantly upon knockdown of TUT7/4/2 (**$p < 0.01$, paired one-tailed t test). SDs are from four independent experiments.

(D) Phylogenetic distribution of the let-7 miRNAs in metazoans. Group II let-7 is conserved in chordates (gray box), whereas group I let-7 is present in all bilaterians, suggesting that group II let-7 may have duplicated and diverged from ancient group I let-7. Precursor structures of all let-7 miRNAs expressed in metazoans were analyzed. See also Figure S6.

According to the deep sequencing data from 104 different human cell lines that had originated from nine different organs (Table S2), group II let-7 accounts for more than 90% of total let-7 population in most human cell types (Figure 6A, left). We also found that in other vertebrate species, group II let-7 is expressed dominantly over group I (Figure 6A, right). Therefore, mono-uridylation-dependent control of group II let-7 is expected to have a substantial impact on the overall activity of the let-7 family. Consistently, in the mRNA sequencing from TUT7/4/2-depleted HeLa cells, the let-7 target genes (with either one or multiple target sites) were upregulated, whereas nontarget genes remained unaffected (Figure 6B, left). In addition, only the let-7 target genes were derepressed, whereas targets of other miRNAs did not change significantly (Figure 6B, right). We also validated the increase of known let-7 targets (HMGA2 and NRAS) by quantitative RT-PCR upon TUT knockdown (Figure 6C). Thus, TUT7/4/2 are necessary to maintain the functionality of let-7.

The structure and sequences of group II let-7 precursors are conserved in chordates (including vertebrates, tunicates, and cephalochordates), suggesting that group II may have evolved in the common ancestor of chordates (Figures 6D and S6A). Group I let-7 loci are found in all bilaterian animals and seem more ancient than group II. However, there are more group II let-7 loci than group I loci in vertebrates, implying that group II may have expanded more rapidly than group I in vertebrates (Bompfünewerer et al., 2005; Roush and Slack, 2008). Thus, group II is dominant over group I in vertebrates, not only in terms of expression levels but also in gene numbers, suggesting that group II let-7 may have played an important role during vertebrate evolution. Of note, TUT7/4/2 homologs are found in all examined vertebrate species (Figure S6B).

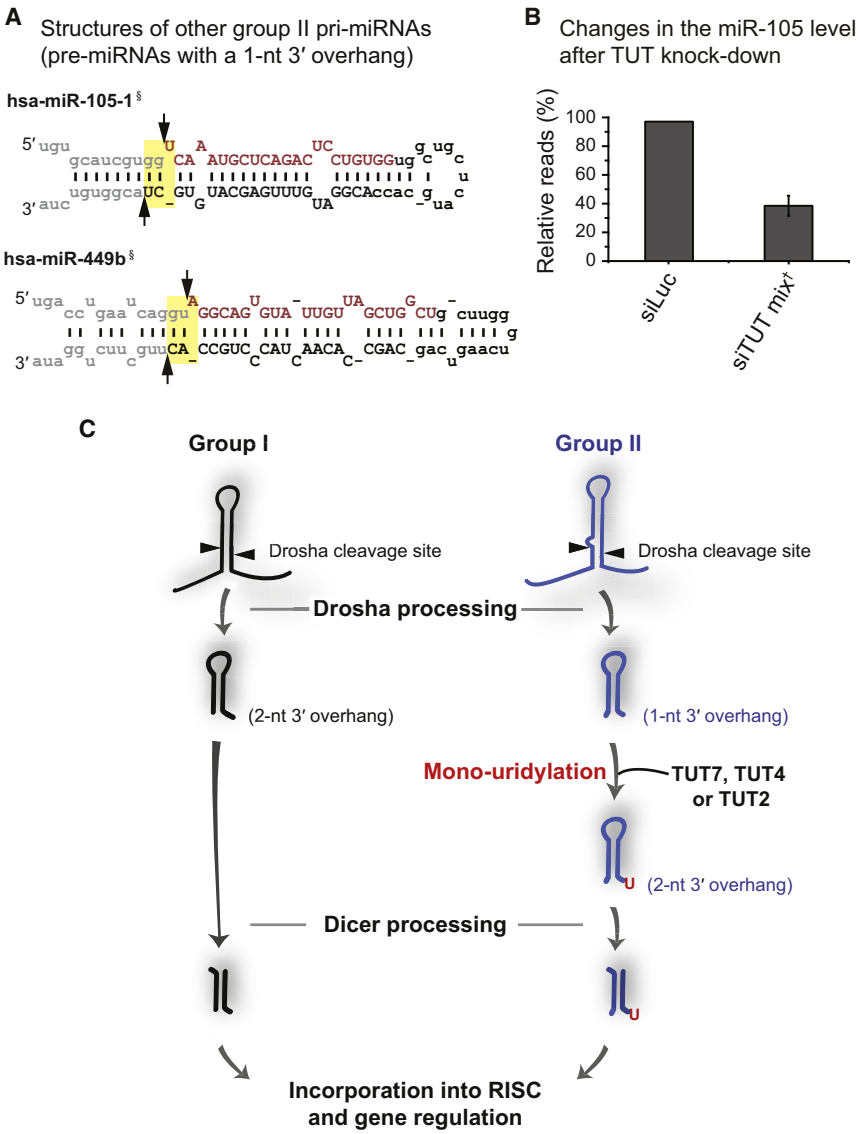

Figure 7. Mono-Uridylation is an Integral Step for Group II miRNA Biogenesis

(A) Pri-miRNA structure of human miR-105 and miR-449b, which are group II miRNA candidates. Mature miRNA sequences are in uppercase with red (miRNA-5p) or black (miRNA-3p). Arrows indicate Drosha processing sites. §Indicates reannotation of Drosha cleavage site according to our analysis. See also Figure S7A.

(B) miR-105 decreased in deep sequencing libraries from TUT-depleted HeLa, implying that miR-105 may also require the TUTs for its efficient maturation. Reads per million (RPM) of miR-105 in siTUT mix-treated cells were compared to that in control cells. Error bars indicate SDs from biological duplicates.

(C) Unlike typical pre-miRNAs that have a 2 nt overhang at the 3′ end (group I), group II pre-miRNAs acquire a 1 nt 3′ overhang end structure because of a bulged nucleotide next to Drosha cleavage site. TUT7, TUT4, and TUT2 redundantly carry out mono-uridylation of group II pre-miRNAs, transforming them to optimal substrates for Dicer cleavage.

DISCUSSION

In conclusion, we identified TUT7, TUT4, and TUT2 as novel components of the miRNA biogenesis pathway (see Figure 7C for a model). TUT7/4/2 mono-uridylate group II pre-miRNAs and thereby play an integral part in group II miRNA maturation. It is interesting that TUT7/4/2 specifically recognize a 1 nt 3′ overhang structure and transfer only one U residue to the 3′ end. This property enables TUTs to reshape the dsRNA end structure to provide optimal substrates for Dicer processing. Because TUT4 interacts only transiently with pre-let-7a-1 (Yeom et al., 2011), the duration of the interaction may be just long enough to transfer one nucleotide. After the first uridylation event, TUTs may dissociate quickly and cannot rebind to the RNA because of the low affinity toward the 2 nt overhang. It will be of interest to investigate the molecular basis of the specific recognition of the end structure by TUT7/4/2.

Our study highlights the importance of the 2 nt 3′ overhang structure in miRNA biogenesis. Drosha talks to the downstream factors (particularly Dicer) by creating the 2 nt 3′ overhang structure that marks the RNAs involved in the miRNA pathway. This is an intriguing example of two physically separated enzymes communicating through an RNA motif. The dependence on 2 nt 3′ overhang streamlines the miRNA maturation pathway and also offers a ground for regulation through pre-miRNA uridylation. It will be interesting to understand how Dicer distinguishes exquisitely the subtle difference in the overhang structure. Structural analysis of vertebrate Dicer protein will be necessary as the only published structure of Dicer is from *Giardia intestinalis*, which does not have canonical miRNA pathway (Macrae et al., 2006). *Giardia* Dicer does not possess a preference for the 2 nt 3′ overhang structure (MacRae et al., 2007; Park et al., 2011).

miRNAs can be classified into group I and group II, based upon the end structure of pre-miRNA and the dependence on mono-uridylation. It is currently unclear which miRNAs outside the let-7 family belong to group II. But based on secondary structure prediction, the pri-miRNAs of miR-105 and miR-449b have a bulged nucleotide next to the Drosha cleavage site, suggesting that the precursors may acquire a 1 nt 3′ overhang structure from Drosha cleavage (Figures 7A and S7A). Deep sequencing data from 104 different human cells (Table S2) indicated that miR-105-3p and miR-449b-3p are frequently mono-uridylated (Figure S7A). Furthermore, the miR-105 level, albeit very low, decreased considerably in HeLa cells after TUT

knockdown, suggesting that miR-105 is a bona fide member of group II (Figure 7B). The level of miR-449b was below detection limit in HeLa cells. Further investigation will be needed to identify additional group II members.

Our data suggest that the group I pre-let-7 is rarely uridylated both in HeLa cells and in vitro assays. In addition, although mono-uridylation has been observed on other group I pre-miRNAs (Newman et al., 2011), the frequency of such uridylation was low and the functional significance of the modification is unclear. Group I miRNAs remained largely unaffected upon TUT7/4/2 depletion in our experiments (Figures 4C and S4C). Thus, although it is possible that other TUTases may control group I miRNAs in certain conditions or cell types, mono-uridylation of group I pre-miRNAs may not be frequent enough to exert a meaningful effect in HeLa cells.

TUT7/4/2 mediate mono-uridylation of pre-let-7 in cells lacking Lin28 and thereby facilitate Dicer processing and compete with exonucleases. This mechanism would effectively shift the balance in favor of biogenesis in the absence of Lin28. Because uridylation is generally associated with RNA degradation (Ji and Chen, 2012; Kim et al., 2010; Ren et al., 2012; Wickens and Kwak, 2008; Wilusz and Wilusz, 2008; Zhao et al., 2012), it was unexpected that TUT knockdown resulted in an increase of trimmed pre-let-7 (Figure 2D), providing an intriguing case where uridylation may have a protective effect.

We have recently reported that Lin28 increases the dwelling time of TUT4 on pre-let-7 (Yeom et al., 2011). Thus, Lin28 enhances the processivity of TUT4 to induce oligo-uridylation, which in turn blocks Dicer processing and facilitates pre-let-7 decay (Hagan et al., 2009; Heo et al., 2008, 2009). Therefore, Lin28 serves as a molecular switch that converts TUT4 (and TUT7) from key biogenesis factors into negative regulators (Figure S7B). Our study unveils two opposing functions of TUTs in miRNA biogenesis. The functional duality of uridylation may contribute to the tight control of let-7 expression during developmental transition and tumorigenesis.

EXPERIMENTAL PROCEDURES

Pre-let-7 Sequencing

Twenty to fifty micrograms of HeLa total RNA were resolved on 15% urea-polyacrylamide gel and RNAs of 50–100 nt were gel purified. Size-fractionated RNAs were ligated to 3′ adaptor by using T4 RNA ligase 2, truncated K227Q (NEB). The ligated RNAs were reverse transcribed with a RT primer that is complementary to the 3′ adaptor by using superscript II (Life Technologies), followed by PCR amplification with the RT primer and a let-7a-specific (or let-7c-specific) forward primer that contains BanI restriction enzyme sites. Because of sequence similarities, the forward primers can hybridize to other let-7 members. The PCR products were cleaved by using BanI (NEB) and then concatamerized by using T4 DNA ligase (NEB). The concatamerized DNAs were cloned for Sanger-sequencing. The sequences of 3′ adaptor and primers are listed in Table S5.

Immunoprecipitation and In Vitro Uridylation

For immunoprecipitation of Flag-TUTases, HEK293T cells were collected 48 hr after transfection with Flag-TUTase expression plasmids. The cells were incubated in Buffer D (200 mM KCl, 10 mM Tris-HCl [pH8.0], 0.2 mM EDTA) for 20 min followed by sonication on ice and centrifugation twice for 15 min at 4°C. The supernatant was incubated with 5 μl of anti-Flag antibody-conjugated agarose beads (anti-Flag M2 affinity gel, Sigma) with constant rotation for 1 hr at 4°C. The beads were washed six times with Buffer D. In vitro uridylation reaction was performed in a total volume of 30 μl in 3.2 mM $MgCl_2$, 1 mM DTT, 0.25 mM UTP, 5′ end labeled pre-miRNA or dsRNA of 1×10^4 to 1×10^5 cpm, and 15 μl of immunopurified proteins on beads (Figures 1 and S1) or 3× Flag-peptide (Sigma) eluted proteins (Figures 5 and S5) in Buffer D. The reaction mixture was incubated at 37°C for 10 (Figures 5 and S5) or 20 min (Figures 1 and S1). The RNA was purified from the reaction mixture by phenol extraction and run on 6% urea polyacrylamide sequencing gel (20 × 40 cm, 0.4 mm thick) at constant 1500 V for 2 hr. Unmodified and mono-uridylated form of pre-let-7 (let-7a-1, b, and c) and dsRNAs were synthesized by ST Pharm. The pre-miRNAs or dsRNAs were radio-labeled at the 5′ end with T4 polynucleotide kinase (Takara) and (γ-32P) ATP. The sequences of pre-miRNAs and dsRNAs are listed in Table S5.

mRNA Library Preparation

mRNAs were purified from total RNA by using Dynabeads mRNA Purification Kit (Life Technologies, 61011). Purified mRNAs were fragmented by RNA Fragmentation Reagents (Life Technologies, AM8740). After fragmentation, phosphate group at 3′ end was removed by Antarctic phosphatase (NEB, M0289L), and RNAs were 5′ phosphorylated by T4 PNK (NEB). Directional and multiplexed mRNA libraries were generated by using TruSeq Small RNA Sample Preparation Kit (Illumina, RS-200–0012) and sequenced by using Illumina HiSeq 2000.

Phylogenetic Analysis of the Structures of let-7 Precursor

All sequences and structures of the let-7 stem-loop in bilaterians were downloaded from miRBase release 18 and UCSC genome browser. The end structures of each pre-let-7 were manually classified into group I and group II. The phylogenetic tree illustrated in Figure 6D was modified from the earlier studies (Niwa and Slack, 2007; Pasquinelli et al., 2003, 2000) and miRBase 18. The full genus and species names are as follows: *Homo sapiens*, *Mus musculus*, *Gallus gallus*, *Xenopus tropicalis*, *Danio rerio*, *Ciona intestinalis*, *Branchiostoma floridae*, *Saccoglossus kowalevskii*, *Strongylocentrotus purpuratus*, *Drosophila melanogaster*, *Caenorhabditis elegans*, *Capitella teleta*, *Lottia gigantean*, *Echinococcus granulosus*, *Nematostella vectensis*, and *Ophlitaspongia tenuis.*

ACCESSION NUMBERS

The GEO accession number for the small RNA sequencing and mRNA sequencing data is GSE40236.

SUPPLEMENTAL INFORMATION

Supplemental Information includes Extended Experimental Procedures, seven figures, and five tables and can be found with this article online at http://dx.doi.org/10.1016/j.cell.2012.09.022.

ACKNOWLEDGMENTS

We are grateful to the members of our laboratory, particularly Joha Park, Hyerim Yi, Dr. Kyu-Hyeon Yeom, Dr. Yoosik Kim, Ahyoung Cho, and Yun Cheng Chang for discussion and technical help. We thank Dr. Yun-jeong Kim and Dr. Daehyun Baek for help in preparation of mRNA sequencing libraries. This work was supported by the Research Center Program (EM1202) of IBS (Institute for Basic Science); the BK21 Research Fellowships (J.L., J.-E.P., and H.C.) from the Ministry of Education, Science and Technology of Korea; and the National Honor Scientist Program (20100020415) through the National Research Foundation of Korea (NRF).

Received: March 27, 2012
Revised: June 26, 2012
Accepted: August 15, 2012
Published online: October 11, 2012

REFERENCES

Balzer, E., and Moss, E.G. (2007). Localization of the developmental timing regulator Lin28 to mRNP complexes, P-bodies and stress granules. RNA Biol. *4*, 16–25.

Bernstein, E., Caudy, A.A., Hammond, S.M., and Hannon, G.J. (2001). Role for a bidentate ribonuclease in the initiation step of RNA interference. Nature *409*, 363–366.

Bohnsack, M.T., Czaplinski, K., and Gorlich, D. (2004). Exportin 5 is a RanGTP-dependent dsRNA-binding protein that mediates nuclear export of pre-miRNAs. RNA *10*, 185–191.

Bompfünewerer, A.F., Flamm, C., Fried, C., Fritzsch, G., Hofacker, I.L., Lehmann, J., Missal, K., Mosig, A., Müller, B., Prohaska, S.J., et al. (2005). Evolutionary patterns of non-coding RNAs. Theory Biosci. *123*, 301–369.

Burns, D.M., D'Ambrogio, A., Nottrott, S., and Richter, J.D. (2011). CPEB and two poly(A) polymerases control miR-122 stability and p53 mRNA translation. Nature *473*, 105–108.

Burroughs, A.M., Ando, Y., de Hoon, M.J., Tomaru, Y., Nishibu, T., Ukekawa, R., Funakoshi, T., Kurokawa, T., Suzuki, H., Hayashizaki, Y., and Daub, C.O. (2010). A comprehensive survey of 3′ animal miRNA modification events and a possible role for 3′ adenylation in modulating miRNA targeting effectiveness. Genome Res. *20*, 1398–1410.

Büssing, I., Slack, F.J., and Grosshans, H. (2008). let-7 microRNAs in development, stem cells and cancer. Trends Mol. Med. *14*, 400–409.

Chiang, H.R., Schoenfeld, L.W., Ruby, J.G., Auyeung, V.C., Spies, N., Baek, D., Johnston, W.K., Russ, C., Luo, S., Babiarz, J.E., et al. (2010). Mammalian microRNAs: experimental evaluation of novel and previously annotated genes. Genes Dev. *24*, 992–1009.

Denli, A.M., Tops, B.B., Plasterk, R.H., Ketting, R.F., and Hannon, G.J. (2004). Processing of primary microRNAs by the Microprocessor complex. Nature *432*, 231–235.

Gregory, R.I., Yan, K.P., Amuthan, G., Chendrimada, T., Doratotaj, B., Cooch, N., and Shiekhattar, R. (2004). The Microprocessor complex mediates the genesis of microRNAs. Nature *432*, 235–240.

Grishok, A., Pasquinelli, A.E., Conte, D., Li, N., Parrish, S., Ha, I., Baillie, D.L., Fire, A., Ruvkun, G., and Mello, C.C. (2001). Genes and mechanisms related to RNA interference regulate expression of the small temporal RNAs that control C. elegans developmental timing. Cell *106*, 23–34.

Grosshans, H., Johnson, T., Reinert, K.L., Gerstein, M., and Slack, F.J. (2005). The temporal patterning microRNA let-7 regulates several transcription factors at the larval to adult transition in C. elegans. Dev. Cell *8*, 321–330.

Guo, Y., Chen, Y., Ito, H., Watanabe, A., Ge, X., Kodama, T., and Aburatani, H. (2006). Identification and characterization of lin-28 homolog B (LIN28B) in human hepatocellular carcinoma. Gene *384*, 51–61.

Hagan, J.P., Piskounova, E., and Gregory, R.I. (2009). Lin28 recruits the TUTase Zcchc11 to inhibit let-7 maturation in mouse embryonic stem cells. Nat. Struct. Mol. Biol. *16*, 1021–1025.

Hammond, S.M., Boettcher, S., Caudy, A.A., Kobayashi, R., and Hannon, G.J. (2001). Argonaute2, a link between genetic and biochemical analyses of RNAi. Science *293*, 1146–1150.

Han, J., Lee, Y., Yeom, K.H., Kim, Y.K., Jin, H., and Kim, V.N. (2004). The Drosha-DGCR8 complex in primary microRNA processing. Genes Dev. *18*, 3016–3027.

Han, J., Lee, Y., Yeom, K.H., Nam, J.W., Heo, I., Rhee, J.K., Sohn, S.Y., Cho, Y., Zhang, B.T., and Kim, V.N. (2006). Molecular basis for the recognition of primary microRNAs by the Drosha-DGCR8 complex. Cell *125*, 887–901.

Heo, I., Joo, C., Cho, J., Ha, M., Han, J., and Kim, V.N. (2008). Lin28 mediates the terminal uridylation of let-7 precursor MicroRNA. Mol. Cell *32*, 276–284.

Heo, I., Joo, C., Kim, Y.K., Ha, M., Yoon, M.J., Cho, J., Yeom, K.H., Han, J., and Kim, V.N. (2009). TUT4 in concert with Lin28 suppresses microRNA biogenesis through pre-microRNA uridylation. Cell *138*, 696–708.

Hutvágner, G., McLachlan, J., Pasquinelli, A.E., Bálint, E., Tuschl, T., and Zamore, P.D. (2001). A cellular function for the RNA-interference enzyme Dicer in the maturation of the let-7 small temporal RNA. Science *293*, 834–838.

Ji, L., and Chen, X. (2012). Regulation of small RNA stability: methylation and beyond. Cell Res. *22*, 624–636.

Jones, M.R., Quinton, L.J., Blahna, M.T., Neilson, J.R., Fu, S., Ivanov, A.R., Wolf, D.A., and Mizgerd, J.P. (2009). Zcchc11-dependent uridylation of microRNA directs cytokine expression. Nat. Cell Biol. *11*, 1157–1163.

Katoh, T., Sakaguchi, Y., Miyauchi, K., Suzuki, T., Kashiwabara, S., Baba, T., and Suzuki, T. (2009). Selective stabilization of mammalian microRNAs by 3′ adenylation mediated by the cytoplasmic poly(A) polymerase GLD-2. Genes Dev. *23*, 433–438.

Ketting, R.F., Fischer, S.E., Bernstein, E., Sijen, T., Hannon, G.J., and Plasterk, R.H. (2001). Dicer functions in RNA interference and in synthesis of small RNA involved in developmental timing in C. elegans. Genes Dev. *15*, 2654–2659.

Kim, V.N., Han, J., and Siomi, M.C. (2009). Biogenesis of small RNAs in animals. Nat. Rev. Mol. Cell Biol. *10*, 126–139.

Kim, Y.K., Heo, I., and Kim, V.N. (2010). Modifications of small RNAs and their associated proteins. Cell *143*, 703–709.

Knight, S.W., and Bass, B.L. (2001). A role for the RNase III enzyme DCR-1 in RNA interference and germ line development in Caenorhabditis elegans. Science *293*, 2269–2271.

Landthaler, M., Yalcin, A., and Tuschl, T. (2004). The human DiGeorge syndrome critical region gene 8 and Its D. melanogaster homolog are required for miRNA biogenesis. Curr. Biol. *14*, 2162–2167.

Lee, Y., Ahn, C., Han, J., Choi, H., Kim, J., Yim, J., Lee, J., Provost, P., Rådmark, O., Kim, S., and Kim, V.N. (2003). The nuclear RNase III Drosha initiates microRNA processing. Nature *425*, 415–419.

Loughlin, F.E., Gebert, L.F., Towbin, H., Brunschweiger, A., Hall, J., and Allain, F.H. (2012). Structural basis of pre-let-7 miRNA recognition by the zinc knuckles of pluripotency factor Lin28. Nat. Struct. Mol. Biol. *19*, 84–89.

Lund, E., Güttinger, S., Calado, A., Dahlberg, J.E., and Kutay, U. (2004). Nuclear export of microRNA precursors. Science *303*, 95–98.

Macrae, I.J., Zhou, K., Li, F., Repic, A., Brooks, A.N., Cande, W.Z., Adams, P.D., and Doudna, J.A. (2006). Structural basis for double-stranded RNA processing by Dicer. Science *311*, 195–198.

MacRae, I.J., Zhou, K., and Doudna, J.A. (2007). Structural determinants of RNA recognition and cleavage by Dicer. Nat. Struct. Mol. Biol. *14*, 934–940.

Martin, G., and Keller, W. (2007). RNA-specific ribonucleotidyl transferases. RNA *13*, 1834–1849.

Meneely, P.M., and Herman, R.K. (1979). Lethals, steriles and deficiencies in a region of the X chromosome of Caenorhabditis elegans. Genetics *92*, 99–115.

Mourelatos, Z., Dostie, J., Paushkin, S., Sharma, A., Charroux, B., Abel, L., Rappsilber, J., Mann, M., and Dreyfuss, G. (2002). miRNPs: a novel class of ribonucleoproteins containing numerous microRNAs. Genes Dev. *16*, 720–728.

Nakanishi, T., Kubota, H., Ishibashi, N., Kumagai, S., Watanabe, H., Yamashita, M., Kashiwabara, S., Miyado, K., and Baba, T. (2006). Possible role of mouse poly(A) polymerase mGLD-2 during oocyte maturation. Dev. Biol. *289*, 115–126.

Nam, Y., Chen, C., Gregory, R.I., Chou, J.J., and Sliz, P. (2011). Molecular basis for interaction of let-7 microRNAs with Lin28. Cell *147*, 1080–1091.

Newman, M.A., Thomson, J.M., and Hammond, S.M. (2008). Lin-28 interaction with the Let-7 precursor loop mediates regulated microRNA processing. RNA *14*, 1539–1549.

Newman, M.A., Mani, V., and Hammond, S.M. (2011). Deep sequencing of microRNA precursors reveals extensive 3′ end modification. RNA *17*, 1795–1803.

Niwa, R., and Slack, F.J. (2007). The evolution of animal microRNA function. Curr. Opin. Genet. Dev. *17*, 145–150.

Park, J.E., Heo, I., Tian, Y., Simanshu, D.K., Chang, H., Jee, D., Patel, D.J., and Kim, V.N. (2011). Dicer recognizes the 5′ end of RNA for efficient and accurate processing. Nature *475*, 201–205.

Pasquinelli, A.E., Reinhart, B.J., Slack, F., Martindale, M.Q., Kuroda, M.I., Maller, B., Hayward, D.C., Ball, E.E., Degnan, B., Müller, P., et al. (2000). Conservation of the sequence and temporal expression of let-7 heterochronic regulatory RNA. Nature *408*, 86–89.

Pasquinelli, A.E., McCoy, A., Jiménez, E., Saló, E., Ruvkun, G., Martindale, M.Q., and Baguñà, J. (2003). Expression of the 22 nucleotide let-7 heterochronic RNA throughout the Metazoa: a role in life history evolution? Evol. Dev. *5*, 372–378.

Piskounova, E., Polytarchou, C., Thornton, J.E., LaPierre, R.J., Pothoulakis, C., Hagan, J.P., Iliopoulos, D., and Gregory, R.I. (2011). Lin28A and Lin28B inhibit let-7 microRNA biogenesis by distinct mechanisms. Cell *147*, 1066–1079.

Polesskaya, A., Cuvellier, S., Naguibneva, I., Duquet, A., Moss, E.G., and Harel-Bellan, A. (2007). Lin-28 binds IGF-2 mRNA and participates in skeletal myogenesis by increasing translation efficiency. Genes Dev. *21*, 1125–1138.

Reinhart, B.J., Slack, F.J., Basson, M., Pasquinelli, A.E., Bettinger, J.C., Rougvie, A.E., Horvitz, H.R., and Ruvkun, G. (2000). The 21-nucleotide let-7 RNA regulates developmental timing in Caenorhabditis elegans. Nature *403*, 901–906.

Ren, G., Chen, X., and Yu, B. (2012). Uridylation of miRNAs by hen1 suppressor1 in Arabidopsis. Curr. Biol. *22*, 695–700.

Richards, M., Tan, S.P., Tan, J.H., Chan, W.K., and Bongso, A. (2004). The transcriptome profile of human embryonic stem cells as defined by SAGE. Stem Cells *22*, 51–64.

Rouhana, L., Wang, L., Buter, N., Kwak, J.E., Schiltz, C.A., Gonzalez, T., Kelley, A.E., Landry, C.F., and Wickens, M. (2005). Vertebrate GLD2 poly(A) polymerases in the germline and the brain. RNA *11*, 1117–1130.

Roush, S., and Slack, F.J. (2008). The let-7 family of microRNAs. Trends Cell Biol. *18*, 505–516.

Rybak, A., Fuchs, H., Smirnova, L., Brandt, C., Pohl, E.E., Nitsch, R., and Wulczyn, F.G. (2008). A feedback loop comprising lin-28 and let-7 controls pre-let-7 maturation during neural stem-cell commitment. Nat. Cell Biol. *10*, 987–993.

Stevenson, A.L., and Norbury, C.J. (2006). The Cid1 family of non-canonical poly(A) polymerases. Yeast *23*, 991–1000.

Tabara, H., Sarkissian, M., Kelly, W.G., Fleenor, J., Grishok, A., Timmons, L., Fire, A., and Mello, C.C. (1999). The rde-1 gene, RNA interference, and transposon silencing in C. elegans. Cell *99*, 123–132.

Tian, B., Bevilacqua, P.C., Diegelman-Parente, A., and Mathews, M.B. (2004). The double-stranded-RNA-binding motif: interference and much more. Nat. Rev. Mol. Cell Biol. *5*, 1013–1023.

Vermeulen, A., Behlen, L., Reynolds, A., Wolfson, A., Marshall, W.S., Karpilow, J., and Khvorova, A. (2005). The contributions of dsRNA structure to Dicer specificity and efficiency. RNA *11*, 674–682.

Viswanathan, S.R., Daley, G.Q., and Gregory, R.I. (2008). Selective blockade of microRNA processing by Lin28. Science *320*, 97–100.

Wickens, M., and Kwak, J.E. (2008). Molecular biology. A tail tale for U. Science *319*, 1344–1345.

Wilusz, C.J., and Wilusz, J. (2008). New ways to meet your (3′) end oligouridylation as a step on the path to destruction. Genes Dev. *22*, 1–7.

Wu, H., Ye, C., Ramirez, D., and Manjunath, N. (2009). Alternative processing of primary microRNA transcripts by Drosha generates 5′ end variation of mature microRNA. PLoS ONE *4*, e7566.

Wyman, S.K., Knouf, E.C., Parkin, R.K., Fritz, B.R., Lin, D.W., Dennis, L.M., Krouse, M.A., Webster, P.J., and Tewari, M. (2011). Post-transcriptional generation of miRNA variants by multiple nucleotidyl transferases contributes to miRNA transcriptome complexity. Genome Res. *21*, 1450–1461.

Yang, D.H., and Moss, E.G. (2003). Temporally regulated expression of Lin-28 in diverse tissues of the developing mouse. Gene Expr. Patterns *3*, 719–726.

Yeom, K.H., Heo, I., Lee, J., Hohng, S., Kim, V.N., and Joo, C. (2011). Single-molecule approach to immunoprecipitated protein complexes: insights into miRNA uridylation. EMBO Rep. *12*, 690–696.

Yi, R., Qin, Y., Macara, I.G., and Cullen, B.R. (2003). Exportin-5 mediates the nuclear export of pre-microRNAs and short hairpin RNAs. Genes Dev. *17*, 3011–3016.

Zhang, H., Kolb, F.A., Brondani, V., Billy, E., and Filipowicz, W. (2002). Human Dicer preferentially cleaves dsRNAs at their termini without a requirement for ATP. EMBO J. *21*, 5875–5885.

Zhang, H., Kolb, F.A., Jaskiewicz, L., Westhof, E., and Filipowicz, W. (2004). Single processing center models for human Dicer and bacterial RNase III. Cell *118*, 57–68.

Zhao, Y., Yu, Y., Zhai, J., Ramachandran, V., Dinh, T.T., Meyers, B.C., Mo, B., and Chen, X. (2012). The Arabidopsis nucleotidyl transferase HESO1 uridylates unmethylated small RNAs to trigger their degradation. Curr. Biol. *22*, 689–694.

Zhu, H., Shah, S., Shyh-Chang, N., Shinoda, G., Einhorn, W.S., Viswanathan, S.R., Takeuchi, A., Grasemann, C., Rinn, J.L., Lopez, M.F., et al. (2010). Lin28a transgenic mice manifest size and puberty phenotypes identified in human genetic association studies. Nat. Genet. *42*, 626–630.

Zhu, H., Shyh-Chang, N., Segrè, A.V., Shinoda, G., Shah, S.P., Einhorn, W.S., Takeuchi, A., Engreitz, J.M., Hagan, J.P., Kharas, M.G., et al; DIAGRAM Consortium; MAGIC Investigators. (2011). The Lin28/let-7 axis regulates glucose metabolism. Cell *147*, 81–94.